

Delignified Wood-based Highly Efficient Solar Steam Generation Device *via* Promoting Both Water Transportation and Evaporation

Yuming He,^a Huayang Li,^a Xuelian Guo,^b and Rongbo Zheng^{a,*}

Wood-based solar steam generation holds great promise in alleviating fresh water crises due to its advantages: light absorbability, thermal management, water transpiration, and water evaporation. Although tremendous efforts have been made to improve wood-based solar steam generation devices, they mainly have focused on the optimization of photothermal materials to optimize light absorbability and thermal management to enhance efficiency of steam generation. This research demonstrates that delignified wood (DL-wood) can further improve the efficiency of steam generation *via* increasing both the water transportation and water evaporation. The results show that after placing carbon nanotubes (CNTs) on DL-wood, the efficiency of steam production is higher than that of natural wood coated with CNTs by 20% under ambient sunlight conditions. DL-wood with CNTs has the following advantages: (1) it is stable, available, and easy to extend; (2) it does not pollute the environment and will not cause discoloration or dregs when used; and (3) it is a promising efficiency-enhancing solution for renewable and portable solar power generation.

Keywords: Solar steam generation; Fast water transportation; Fast water evaporation; Delignified wood

Contact information: a: Yunnan Province Key Laboratory of Wood Adhesives and Glued Products, College of Chemical Engineering, Southwest Forestry University, Kunming 650224, P. R. China; b: Wetland College, Southwest Forestry University, Kunming 650224, P. R. China;

* Corresponding author: zhengrbzy@hotmail.com

INTRODUCTION

Solar steam generation is one of the most promising, sustainable techniques for desalination and water purification, and it has attracted great attention (Ghasemi *et al.* 2014; Gamelas and Ferraz 2015; Ito *et al.* 2015). There are four key factors that affect the efficiency of solar generation devices: sunlight absorbability, thermal management, water transportation, and water evaporation (Jin *et al.* 2016; Ni *et al.* 2016; Wang *et al.* 2016a). Various structural materials have been designed and developed for this application (Zielinski *et al.* 2016), such as plasmonic metal particles for localizing heat generation (Wang *et al.* 2016b; Zhou *et al.* 2016a,b), bilayered forms with a black surface for efficient light absorption and thermal management (Li *et al.* 2016; Shi *et al.* 2017), and carbonaceous materials with broadband sunlight absorptivity and hydrophilic surface for water transpiration (Ghasemi *et al.* 2014). More recently, inspired by the water transpiration behavior of trees, the use of carbon nanotube (CNT)-modified horizontally cut wood (Chen *et al.* 2017; Wang, *et al.* 2017), graphite-coated vertically cut wood (Li *et al.* 2018), grapheme oxide-coated wood (Liu *et al.* 2017b), surface carbonization, vertically cut wood (Liu *et al.* 2017a; Xue *et al.* 2017; Zhu *et al.* 2017), and Chinese ink-coated wood (Yang *et al.* 2018) have been demonstrated as efficient solar steam generation devices (Wright *et al.* 2013). This is due to the systematic optimizations of

light absorbability (Jiang *et al.* 2016), thermal management, and water transpiration enabled by the unique structure consisting of a carbonaceous surface as a light absorber, insulating the wood matrix as a thermal blocker and hierarchical micro/nanochannels as a water transportation pathway.

Although the above-mentioned wood-based solar steam generation devices have been demonstrated to greatly enhance the efficiency of solar steam generation, they mainly focused on various photothermal materials such as CNT, graphite, graphene oxide, surface carbonization, and Chinese ink combined with hierarchical porous structures to improve both the sunlight absorbability and the thermal management. There are few reports on enhancing the efficiency of solar steam generation devices *via* improving both the water transportation ability and water evaporation of wood-based devices (Chen *et al.* 2017). Wood cell walls are primarily composed of fiber tracheids and vessels with lumen diameters ranging from 10 to 100 μm , which act as pathways for rapid water transport (Zhong *et al.* 2018a). In wood cell walls, cellulose microfibrils are embedded within lignocellulosic matrices, in which the lignin reinforces the cell walls to improve the mechanical properties and also reduces the permeability of water.

The objective of the current study was to test the hypothesis that the efficiency of solar steam generation devices can be improved by removing lignin from the wood. After the removal of hydrophobic lignin, the delignified wood (DL-wood) not only preserved the original hierarchical structure of wood, but also increased hydrophilicity and possessed more micro/nano pores in the cell walls and cell wall corners, which promotes both water transportation and evaporation from the bottom to the top surface of wood. When the sunlight illustrates the CNTs-coated DL-wood, the black surface will absorb the sunlight and generate localized heat at the water-air interface to evaporate *via* increasing the local temperature (Zhong and Huang 2019). With a sufficient supply of bottom water to the CNTs coated top wood surface (Zheng *et al.* 2016; Zhong *et al.* 2018b) and fast water evaporation, the efficiency of CNTs modified DL-wood device might increase compared with that of CNTs modified natural wood device under ambient sunlight illumination.

This study reports the development of CNTs-modified DL-wood solar steam generation devices by replacing the natural wood with DL-wood, which is obtained by H_2O_2 steam delignification. DL-wood is used as a substrate to be modified with CNTs by cutting along the direction vertical to the growth direction of trees. The water transportation and evaporation rates were characterized by measuring the transport distance of dye aqueous solutions and the mass change of water after illuminating to ambient sunlight. Compared with CNTs modified natural wood device, the efficiency of CNT modified DL-wood devices increased from 60% to 73% in this study.

EXPERIMENTAL

Materials and Chemicals

Basswood slices with a diameter of 4 cm and a thickness of 0.5 cm were used in this study. These samples have the original channels in wood aligned perpendicular to the wood plane. DL-wood was obtained by radially cutting the wood trunk, also called Ra-wood. The chemicals used in removing lignin from wood were hydrogen peroxide (30% solution, Sino pharm, Beijing, China) and CNTs (Sino pharm). The solvents used were ethanol alcohol (Sino pharm) and deionized water.

Delignification of the Wood

The pre-cut wood slices were steam delignified by being placed on grids with the unit size of 5 mm x 5 mm, which was placed about 2 cm above an H₂O₂ boiling aqueous solution (30 wt%) (Li *et al.* 2019). When the yellow color of the sample disappeared (2 to 4 h), the samples were removed and rinsed with cold water and ethanol. The DL-wood samples were stored in ethanol.

Synthesis of DL-wood/CNTs

Commercial CNTs powder was dispersed in acetone to make the CNTs solution. These wood samples were immersed in the solution of CNTs, then taken out and dried in air. This process was repeated several times to coat CNTs to the amount of about 0.4 wt% of wood with different treatments, resulting in the final product of CNTs-coated wood (Zheng *et al.* 2015; Chen *et al.* 2017).

Measurements and Characterizations

The morphologies of the samples were characterized by a scanning electron microscope (SEM, TESCAN VEGA3, Brno, Czech Republic). The lignin contents were measured according to TAPPI T222 om-11 (2011). A universal material machine (ProLine z020tn, Zwick, Ulm, Germany) was used to measure the mechanical properties.

RESULTS AND DISCUSSION

Lignin Content and Properties

The CNTs modified DL-wood solar steam generation device is shown in Fig. 1. First, DL-wood was prepared by delignification of natural basswood *via* H₂O₂ steam. CNTs were coated on the surface of DL-wood. Finally, the device was put on the surface of water in a glass beaker to generate steam under ambient sunlight.

As shown in Fig. 2a, the lignin content of basswood can be decreased from 22.5% (natural wood) to 12.3% (half DL-wood), to 1.01% (DL-wood) when the H₂O₂ steam was prolonged from 2 h to 4 h, respectively. Notably, the delignified wood with 1.01% lignin content was still strong enough to be exploited in the solar steam generation device since the mechanical strength of the DL-wood in wet state and dry state is 0.42 MPa and 4.5 MPa, respectively. The microstructures of the natural and DL-wood were characterized by scanning electron microscopy (SEM). Figure 2c to 2f show the SEM images of the basswood before and after delignification. There are massive lumina with the diameter in the range from 10 μm to 50 μm (Ito *et al.* 2015). High-magnification SEM images reveal that the natural wood possesses dense, smooth cell wall corners and the middle lamella. Compared with natural wood, massive microscale pores were generated in the cell walls and cell wall corners after steam delignification, which promotes the water transportation and evaporation to the top surface (Fig. 2c and 2d).

To investigate the water transportation capacity, a water transportation experiment was designed. As shown in Fig. 3, 5 mm thick of natural wood and DL-wood were put into dye solution to observe the distance dye traveled after a certain time. As shown in Figs. 3c and 3d, the dye in the DL-wood were always transformed upwards by a greater distance, which indicates that the DL-wood has better water transportation capabilities than natural wood.

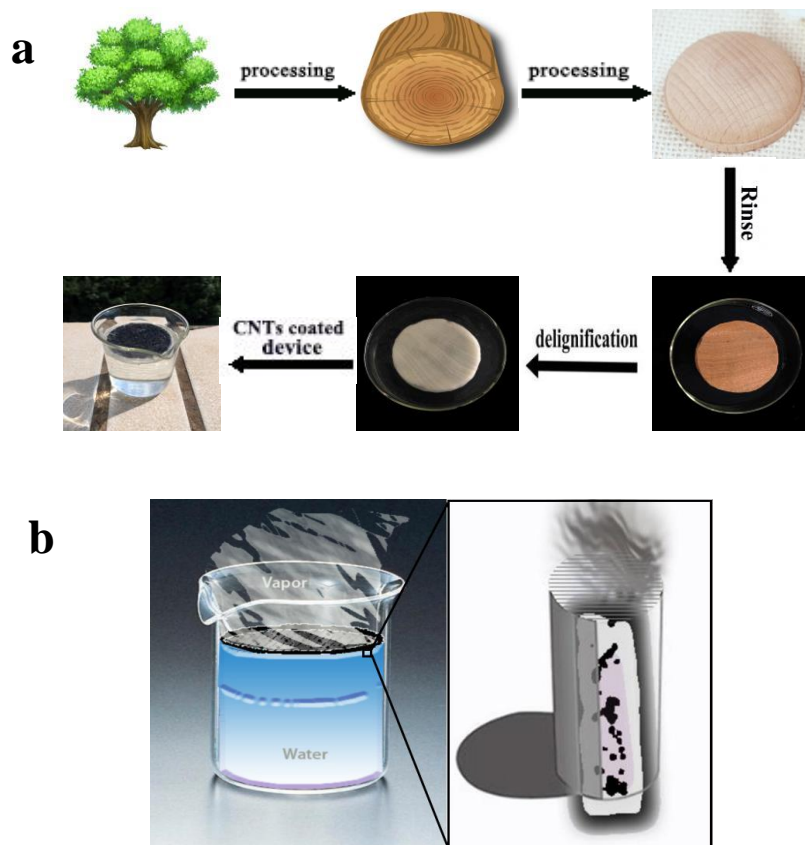


Fig. 1. (a) The preparation process of DL-wood/CNTs. (b) A schematic drawing of an DL-wood/CNTs device that absorbs sunlight and heat to generate water vapor on the surface of the wood and approximate working drawing of a vessel channel, after the water molecules reach the top, the water molecules release rapidly through the local heat provided by the CNTs

To verify the superiority of DL-wood compared with natural wood in the evaporation of water, water-saturated DL-wood and natural wood were placed under 1 sun conditions for self-evaporation. Microholes and smoother vessel channels were generated *via* the removal of hydrophobic lignin, leading to faster evaporation of water under sunlight conditions than natural wood. DL-wood and natural wood were subjected to water self-volatization for 8 cycles under sunny (condition 1) conditions. The water evaporation of DL-wood was $0.261 \text{ kg m}^{-2} \text{ h}^{-1}$, $0.245 \text{ kg m}^{-2} \text{ h}^{-1}$, $0.276 \text{ kg m}^{-2} \text{ h}^{-1}$, $0.267 \text{ kg m}^{-2} \text{ h}^{-1}$, $0.259 \text{ kg m}^{-2} \text{ h}^{-1}$, $0.268 \text{ kg m}^{-2} \text{ h}^{-1}$, $0.250 \text{ kg m}^{-2} \text{ h}^{-1}$, and $0.254 \text{ kg m}^{-2} \text{ h}^{-1}$, while that of natural wood is $0.228 \text{ kg m}^{-2} \text{ h}^{-1}$, $0.220 \text{ kg m}^{-2} \text{ h}^{-1}$, $0.234 \text{ kg m}^{-2} \text{ h}^{-1}$, $0.231 \text{ kg m}^{-2} \text{ h}^{-1}$, $0.225 \text{ kg m}^{-2} \text{ h}^{-1}$, $0.234 \text{ kg m}^{-2} \text{ h}^{-1}$, $0.225 \text{ kg m}^{-2} \text{ h}^{-1}$, $0.223 \text{ kg m}^{-2} \text{ h}^{-1}$, respectively. As shown in Fig. 4b, the enhancement factor of evaporation of DL-wood *vs.* natural wood is 12% to 18%.

Under ambient sunlight (light intensity of 0.98 kW m^{-2} , ambient temperature of $30 \text{ }^{\circ}\text{C}$) for 10 min, the water loss for the blank water control group, the natural wood/CNTs group, the half DL-wood/CNTs group, and the DL-wood/CNTs group were 0.08 kg/m^2 , 0.14 kg/m^2 , 0.17 kg/m^2 , and 0.19 kg/m^2 , respectively. As illustrated in Fig. 4c, after 1 h, the water loss of the blank water control group, the natural wood/CNTs group, the half DL-wood/CNTs group, and the DL-wood/CNTs group were 0.79 kg/m^2 , 1.24 kg/m^2 , 1.31

kg/m², and 1.40 kg/m², respectively.

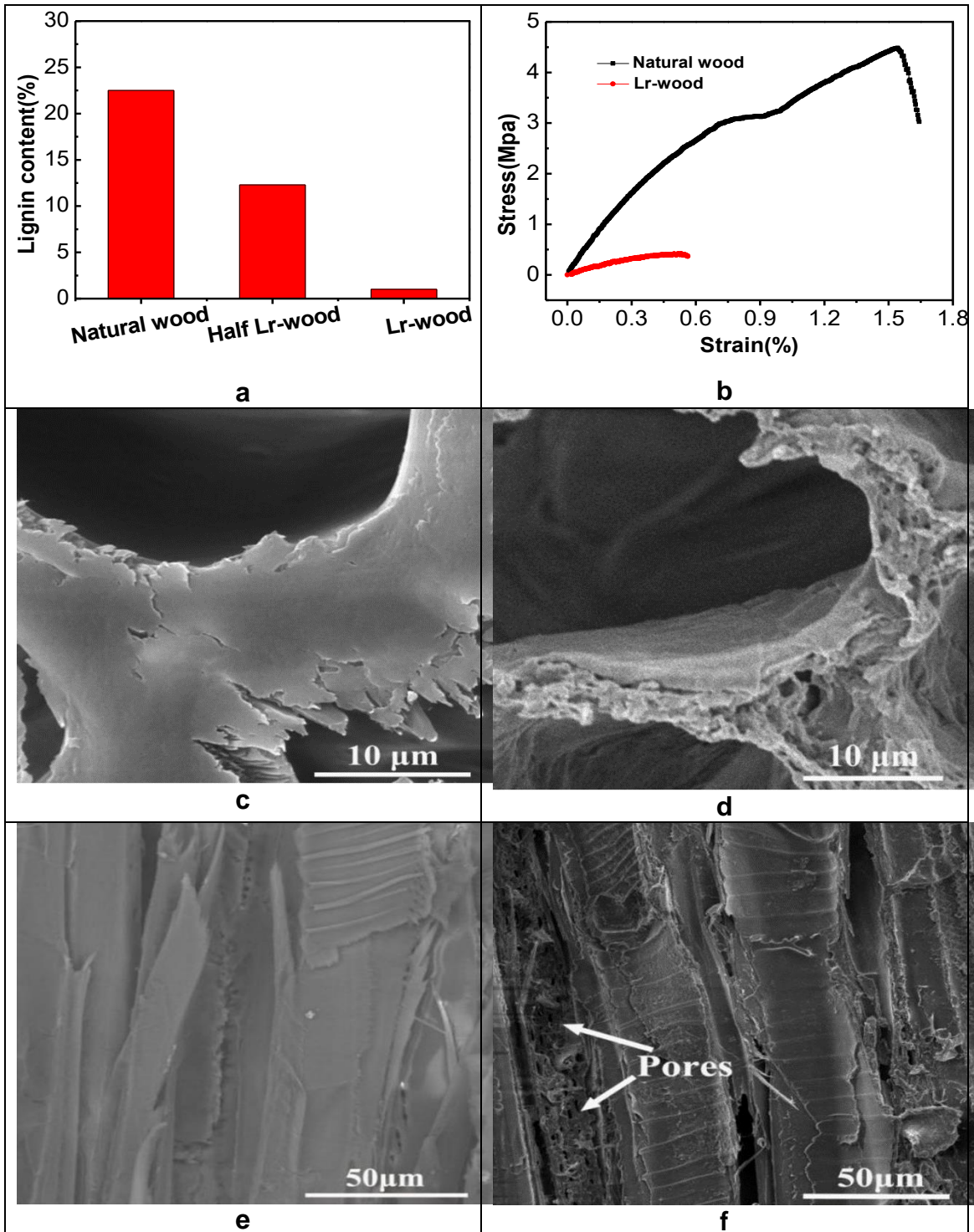


Fig. 2. (a) Lignin content of natural wood, half DL-wood and DL-wood. (b) Experimental stress-strain curves for the DL-wood in wet state. SEM images of (c, e) natural wood and (d, f) DL-wood.

The water evaporation caused by the wind factor was subtracted since the outdoor experiment was influenced by the wind. The steam generation rate of the last four control

groups was summarized as: $0.48 \text{ kg m}^{-2} \text{ h}^{-1}$, $0.94 \text{ kg m}^{-2} \text{ h}^{-1}$, $1.01 \text{ kg m}^{-2} \text{ h}^{-1}$, and $1.12 \text{ kg m}^{-2} \text{ h}^{-1}$. The enhancement factor of evaporation in the last three groups was 1.9 times, 2.1 times, and 2.3 times of that of the blank water group, shown in Fig. 4d.

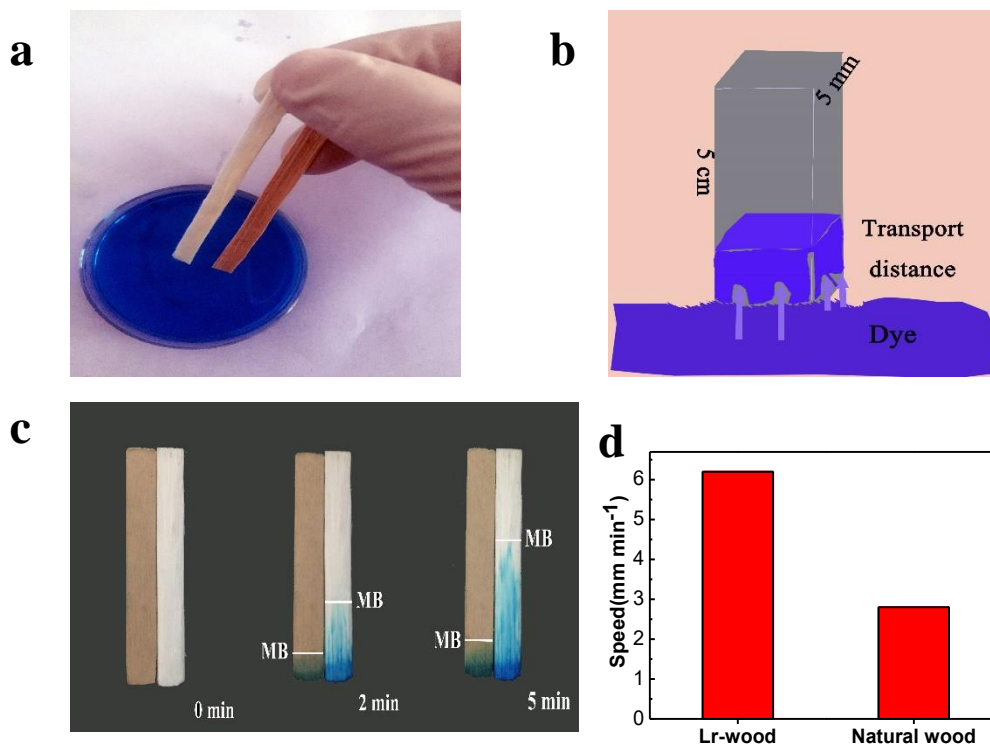


Fig. 3. (a) The experimental sketch and (b) brief comment of Methylene blue solution transport in DL- and natural wood. (c) The solution transport distances between DL- and natural wood for 0 min, 2 min, and 5 min. (d) The average solution transport speed between DL- and natural wood at the end of the 5th min.

The amount of steam production of DL-wood/CNTs was higher than that of natural wood/CNTs by 20% under the same ambient sunlight. It can be seen that under the daytime sun illumination (1 sun), DL-wood/CNTs exhibited good performance for solar steam generation.

Thus, DL-wood/CNTs generated more steam than natural wood/CNTs, which greatly improves the efficiency of solar energy utilization. Under normal sunlight illumination (1 sun), the solar energy efficiency of DL-wood/CNTs devices reached 73%, which was calculated using the following equation (Chen *et al.* 2017),

$$\eta = mh_{LV}/Copt P_0 \quad (1)$$

where m ($\text{kg m}^{-2} \text{ h}^{-1}$) denotes the evaporation rate, $Copt$ is the optical concentration, and h_{LV} is the total enthalpy of the liquid-vapor phase transition including the sensible heat (Chen *et al.* 2017). Compared with the previously reported solar energy utilization rate of 65% under sunlight (1 sun), DL-wood/CNTs increased the efficiency by 8%. This provides a potential, alternative device either steam power production or transmission, and it also opens up new paths for global energy issues that need to be solved. It should be noted that when the light intensity continuously increased from 1 to 10 suns, the steam generation efficiency gradually improved, and the solar energy utilization efficiency gradually improved (Chen *et al.* 2017).

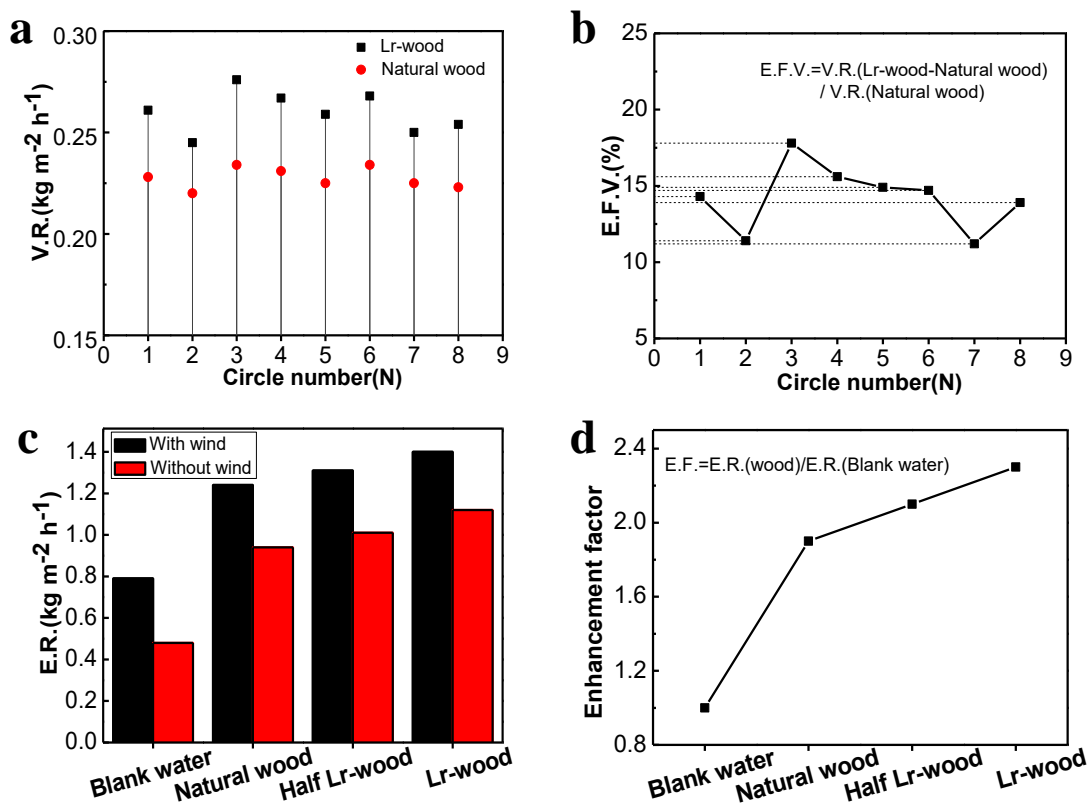


Fig. 4. (a) The volatilization rate (V.R.) of the material under normal daylight (1 sun); (b) the enhancement factor of evaporation of DL-wood vs natural wood; (c) the steam generation efficiency; and (d) the enhancement factor of DL-wood, half DL-wood, natural wood, and blank water control group.

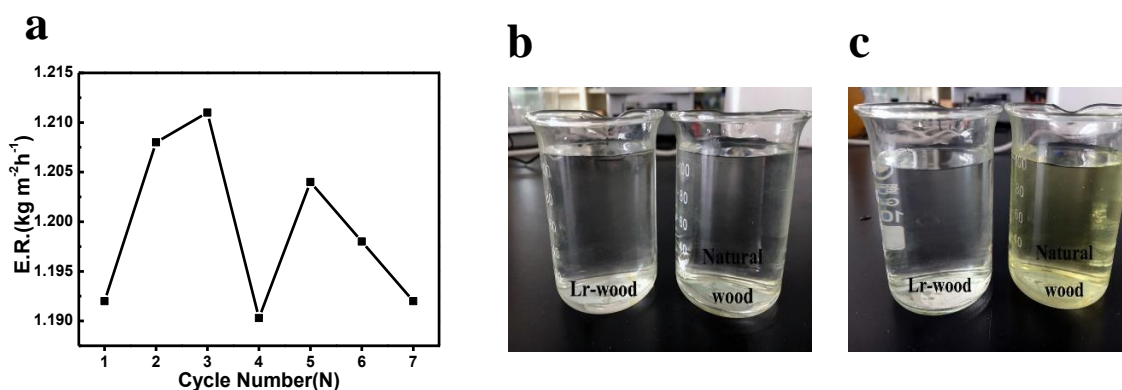


Fig. 5. (a) A cycle diagram of the evaporation rate of the DL-wood-based steam generation. Pictures of DL-wood and Natural Wood Devices (b) before and (c) after use.

To demonstrate the DL-wood-based steam generation stability, a cycle diagram of the evaporation rate is revealed in Fig. 5a. Since the mechanical strength was slightly reduced after the material was wetted, the principle of light handling is followed during use, so DL-wood/CNTs is not damaged and can be recycled. During the seven cycles of recycling, the DL-wood/CNTs device produced steam rates of 1.192 kg m⁻² h⁻¹, 1.208 kg

$\text{m}^{-2} \text{h}^{-1}$, $1.211 \text{ kg m}^{-2} \text{h}^{-1}$, $1.1903 \text{ kg m}^{-2} \text{h}^{-1}$, $1.204 \text{ kg m}^{-2} \text{h}^{-1}$, $1.198 \text{ kg m}^{-2} \text{h}^{-1}$, and $1.192 \text{ kg m}^{-2} \text{h}^{-1}$, respectively. The above data demonstrated the good stability and recyclability of DL-wood/CNTs. Moreover, as seen in Fig. 5b and 5c, the evaporation devices before and after evaporation are shown to verify that DL-wood/CNTs device will not pollute the environment. It can be clearly identified that the solution after evaporation exhibits yellow color due to the leaching of natural wood. However, it is clean and pollution-free for DL-wood, and benign to the environment (He *et al.* 2019).

CONCLUSIONS

1. The steam generation efficiency of delignified wood (DL-wood) was improved in comparison to the default wood by increasing the water transportation and evaporation, which resulted from the removal of most hydrophobic lignin from natural wood. Under ambient sunlight, the steam generation efficiency of DL-wood with carbon nanotubes (CNTs) was about 20% higher than that of natural wood/CNTs.
2. Solar energy utilization of DL-wood/CNTs reached 73% under ambient sunlight. Compared with Hu's (Chen *et al.* 2017), DL-wood/CNTs increased thermal efficiency by 8%.
3. When floating on water, DL-wood/CNTs will not fade so it will not further pollute water sources as natural wood do.
4. DL-wood/CNTs with the advantages of having low cost, simple design, mesoporous structure, and being environmentally friendly is originally proposed for solar steam generation.

ACKNOWLEDGEMENTS

The financial support for this research was provided by the Joint Special Project of Agricultural Basic Research in Yunnan (2017FG001036) and National Natural Science Foundation of China (41563008, 31100420).

REFERENCES CITED

- Chen, C. J., Li, Y., Song, J., Yang, Z., Kuang, Y., Hitz, E., Jia, C., Gong, A., Jiang, F., Zhu, J. Y., Yang, B., Xie, J., and Hu, L. (2017). "Highly flexible and efficient solar steam generation device," *Adv. Mater.* 29(30), 1701756. DOI: 10.1002/adma.201701756
- Gamelas, J. A. F., and Ferraz, E. (2015). "Composite films based on nanocellulose and nanoclay minerals as high strength materials with gas barrier capabilities: Key points and challenges," *BioResources* 10(4), 6310-6313. DOI: 10.15376/biores.10.4.6310-6313
- Ghasemi, H., Ni, G., Marconnet, A. M., Loomis, J., Yerci, S., Miljkovic, N., and Chen, G. (2014). "Solar steam generation by heat localization," *Nat. Commun.* 5(1), 4449. DOI: 10.1038/ncomms5449

- He, Y. M., Li, H. Y., Guo, X. L., and Zheng, R. B. (2019). "Bleached wood supports for floatable, recyclable, and efficient three dimensional photocatalyst," *Catalysts* 9(2), 115. DOI: 10.3390/catal9020115
- Ito, Y., Tanabe, Y., Han, J., Fujita, T., Tanigaki, K., and Chen, M. (2015). "Multifunctional porous graphene for high-efficiency steam generation by heat localization," *Adv. Mater.* 27(29), 4302-4307. DOI: 10.1002/adma.201501832
- Jiang, Q., Tian, L., Liu, K. K., Tadepalli, S., Raliya, R., Biswas, P., Naik, R. R., and Singamaneni, S. (2016). "Bilayered biofoam for highly efficient solar steam generation," *Adv. Mater.* 28(42), 9400-9407. DOI: 10.1002/adma.201601819
- Jin, H., Lin, G., Bai, L., Zeiny, A., and Wen, D. (2016). "Steam generation in a nanoparticle-based solar receiver," *Nano Energy* 28, 397-406. DOI: 10.1016/j.nanoen.2016.08.011
- Li, H., Xu, W., Tang, M., Zhou, L., Zhu, B., Zhu, S., and Zhu, J. (2016). "Graphene oxide-based efficient and scalable solar desalination under one sun with a confined 2D water path," *P. Natl. Acad. Sci. USA* 113(49), 13953-13958. DOI: 10.1073/pnas.1613031113
- Li, H. Y., Guo, X. L., He, Y. M., and Zheng, R. B. (2019). "A green, steam-modified delignification method to low lignin delignified wood for thick, large, highly transparent wood composites," *J. Mater. Res.* 2019. DOI: 10.1557/jmr.2018.466
- Li, T., Liu, H., Zhao, X. P., Chen, G., Dai, J. Q., Pastel, G., Jia, C., Chen, C. J., Hitz, E., Siddhartha, D., Yang, R. G., and Hu, L. B. (2018). "Scalable and highly efficient mesoporous wood-based solar steam generation device: Localized heat, rapid water transport," *Adv. Funct. Mater.* 28(16), 1707134. DOI: 10.1002/adfm.201707134
- Liu, H., Chen, C. J., Chen, G., Kuang, Y. D., Zhao, X. P., Song, J. W., Jia, C., Xu, X., Hitz, E., Xie, H., Wang, S., Jiang, F., Li, T., Li, Y. J., Gong, A., Yang, R. G., Das, S., and Hu, L. B. (2017a). "High-performance solar steam device with layered channels: Artificial tree with a reversed design," *Adv. Energy Mater.* 8, 1701616. DOI: 10.1002/aenm.201701616
- Liu, K., Jiang, Q., Tadepalli, S., Raliya, R., Biswas, P., Naik, R. R., and Singamaneni, S. (2017b). "Wood-graphene oxide composite for highly efficient solar steam generation and desalination," *ACS Appl. Mater. Inter.* 9(8), 7675-7681. DOI: 10.1021/acsami.7b01307
- Ni, G., Li, G., Boriskina, S. V., Li, H., Yang, W., Zhang, T., and Chen, G. (2016). "Steam generation under one sun enabled by a floating structure with thermal concentration," *Nature Energy* 1(9), 16126. DOI: 10.1038/NENERGY.2016.126
- Shi, L., Wang, Y., Zhang, L., and Wang, P. (2017). "Rational design of a bi-layered reduced graphene oxide film on polystyrene foam for solar-driven interfacial water evaporation," *J. Mater. Chem. A* 5(31), 16212-16219. DOI: 10.1039/C6TA09810J
- TAPPI T222 om-11 (2011). "Acid-insoluble lignin in wood and pulp," TAPPI Press, Atlanta, GA.
- Wang, G., Fu, Y., Ma, X., Pi, W., Liu, D., and Wang, X. (2017). "Reusable reduced graphene oxide based double-layer system modified by polyethylenimine for solar steam generation," *Carbon* 114, 117-124. DOI: 10.1016/j.carbon.2016.11.071
- Wang, G., Li, Y., Deng, L., Wei, N., Weng, Y., Dong, S., Qi, D., Qiu, J., Chen, X., and Wu, T. (2016a). "High-performance photothermal conversion of narrow-bandgap Ti_2O_3 nanoparticles," *Adv. Mater.* 29(3), 1603730. DOI: 10.1002/adma.201603730
- Wang, Y., Zhang, L., and Wang, P. (2016b). "Self-floating carbon nanotube membrane on macroporous silica substrate for highly efficient solar-driven interfacial water

- evaporation," *ACS Sustain. Chem. Eng.* 4(3), 1223-1230. DOI: 10.1021/acssuschemeng.5b01274
- Wright, R. S., Bond, B. H., and Chen, Z. (2013). "Steam bending of wood; Embellishments to an ancient technique," *BioResources* 8(4), 4793-4796. DOI: 10.15376/biores.8.4.4793-4796
- Xue, G. B., Liu, K., Chen, Q., Yang, P. H., Li, J., Ding, T. P., Duan, J. J., Qi, B., and Zhou, J. (2017). "Robust and low-cost flame-treated wood for high-performance solar steam generation," *ACS Appl. Mater. Inter.* 9(17), 15052-135057. DOI: 10.1021/acsam.7b01992
- Yang, G. C., Chen, Z. W., Xie, Y. S., Wang, J., Elam, J. W., Li, W. H., and Darling, S. B. (2018). "Chinese ink: A powerful photothermal material for solar steam generation," *Adv. Mater. Interfaces* 1801252. DOI: 10.1002/admi.201801252
- Zheng, R. B., Tshabalala, M. A., Li, Q., and Wang, H. (2015). "Weathering performance of wood coated with a combination of alkoxysilanes and rutile TiO₂ hierarchical nanostructures," *BioResources* 10(4), 7053-7064. DOI: 10.15376/biores.10.4.7053-7064
- Zheng, R. B., Tshabalala, M. A., Li, Q., and Wang, H. (2016). "Photocatalytic degradation of wood coated with a combination of rutile TiO₂ nanostructures and low-surface free-energy materials," *BioResources* 11(1), 2393-2402. DOI:10.15376/biores.11.1.2393-2402
- Zhong, J., Huang, C., Wu, D., and Lin, Z. (2018a). "Influence factors of the evaporation rate of a solar steam generation system: A numerical study," *Int. J. Heat Mass Tran.* 128, 860-864. DOI: 10.1016/j.ijheatmasstransfer.2018.09.079
- Zhong, J., Huang, C., and Wu, D. (2018b). "Surrounding effects on the evaporation efficiency of a bi-layered structure for solar steam generation," *Applied Thermal Engineering* 144, 331-341. DOI: 10.1016/j.applthermaleng.2018.08.074
- Zhong, J., and Huang, C. (2019). "Crowding effects of nanoparticles on energy absorption in solar absorption coatings," *J. Appl. Phys.* 125(3), 033103. DOI: 10.1063/1.5064515
- Zhou, L., Tan, Y., Ji, D., Zhu, B., Zhang, P., Xu, J., Gan, Q., Yu, Z., and Zhu, J. (2016a). "Self-assembly of highly efficient, broadband plasmonic absorbers for solar steam generation," *Science Advances* 2(4), e1501227-e1501227. DOI: 10.1126/sciadv.1501227
- Zhou, L., Tan, Y., Wang, J., Xu, W., Yuan, Y., Cai, W., Zhu, S., and Zhu, J. (2016b). "3D self-assembly of aluminium nanoparticles for plasmon-enhanced solar desalination," *Nat. Photonics* 10(6), 393-398. DOI: 10.1038/NPHOTON.2016.75
- Zhu, M. W., Li, Y. J., Chen, G., Jiang, F., Yang, Z., Luo, X. G., Wang, Y. B., Lacey, S. D., Dai, J. Q., Wang, C. W., Jia, C., Wan, J. Y., Yao, Y. G., Gong, A., Yang, B., Yu, S., Das, Z. F., and Hu, L. B. (2017). "Tree-inspired design for high-efficiency water extraction," *Adv. Mater.* 29(44), 1704107. DOI: 10.1002/adma.201704107
- Zielinski, M. S., Choi, J.-W., Grange, T. La, Modestino, M., Hashemi, S. M. H., Pu, Y., Birkhold, S., Hubbell, J. A., and Psaltis, D. (2016). "Hollow mesoporous plasmonic nanoshells for enhanced solar vapor generation," *Nano Lett.* 16(4), 2159-2167. DOI: 10.1021/acs.nanolett.5b03901

Article submitted: Dec. 10, 2018; Peer review completed: Feb. 17, 2019; Revised version received: March 11, 2019; Accepted: March 16, 2019; Published: March 25, 2019.
DOI: 10.15376/biores.14.2.3758-3767